Microscopic cluster model study of ^{3}He + p scattering

K. Arai*
Division of General Education, Nagaoka National College of Technology, 888 Nishikatakai, Nagaoka, Niigata 940-8532, Japan

S. Aoyama†
Center for Academic Information Service, Niigata University, Niigata 950-2181, Japan

Y. Suzuki‡
Physics Department, Faculty of Science and Graduate School of Science and Technology, Niigata University, Niigata 950-2181, Japan

(Received 3 November 2009; published 15 March 2010)

We calculate the ^{3}He + p scattering phase shifts for the S and P waves in a microscopic cluster model, in which the description of the ^{3}He wave function is extended from a simple $(0s)^3$ model to a three-body model. We employ two different nucleon-nucleon interactions, the Minnesota (MN) and AV8′ potentials, to investigate the role of the $d + 2p$ channel in the low-energy phase shifts. The role of the $d + 2p$ channel in the P-wave phase shifts is very sensitive to the choice of the potential. The $d + 2p$ channel is indispensable in reproducing the resonant phase shifts in the AV8′ potential while it plays a minor role in the MN potential. On the contrary, the role of this channel in the S-wave nonresonant phase shifts is negligible in both potentials.

DOI: 10.1103/PhysRevC.81.037301 PACS number(s): 21.60.Gx, 25.40.Cm, 27.10.+h

For studies of structure and reactions of light nuclei, the cluster model is known to be one of the successful models [1]. A microscopic cluster model such as the resonating group method (RGM) [1] employs two ingredients. The first is to assume that the nucleus is composed of several clusters, where the traditional calculations employ the simple $0\hbar\omega$ cluster wave functions or the superposition of such wave functions. The second is to employ an effective nucleon-nucleon (N-N) interaction such as the Minnesota (MN) potential [2].

The intrinsic wave function of the s-shell cluster is usually approximated with the $0s$ harmonic-oscillator (h.o.) function, whereas the cluster relative motion is solved accurately. Corresponding to the simplified cluster wave functions, only the central, LS, and Coulomb terms of the N-N interaction is usually employed, and the effects of the tensor force and the short-range repulsion that are present in a realistic interaction are presumed to be renormalized in the central force of the effective interaction. Some calculations employ other types of effective N-N interaction, including the tensor force [3,4]. However, because the cluster wave function was kept a simple $0s$ h.o. function, its contribution was considered only for the cluster relative motion.

It is well known that the ground state of ^{4}He, for example, has a large admixture of the D-wave component attributable to the tensor force, amounting to $P_d \approx 14\%$ for the AV8′ potential [5–7]. It was discussed that this D-wave component plays an important role in reproducing the quadrupole moment of the ground state of ^{6}Li [4]. The D-wave component with $(L, S) = (2, 3/2)$ in the ground state of ^{3}He is 8.5% for the AV8′ potential [7].

To understand more deeply the structure and reactions of light nuclei, it is important to develop the microscopic cluster model that employs the more realistic cluster wave functions. The RGM calculation starting from the realistic N-N interaction and the corresponding cluster wave functions built up by the *ab initio* no-core shell model was already developed in Ref. [8]. The purpose of the present article is to develop such calculations in which the cluster wave functions are given by the Gaussian basis functions selected by the stochastic variational method (SVM) [9,10] and to see the effects on the ^{3}He + p S- and P-wave elastic scatterings. The ^{3}He cluster wave function is extended from the $(0s)^3$ h.o. function to the $p + p + n$ three-body wave function. We have tested this extended model with two different N-N interactions: One is a conventional effective interaction, the MN potential, and the other is a realistic interaction, the AV8′ potential.

Four P-wave broad resonances with spin and parity 2^-, 1^-, 0^-, and 1^- are observed in the low-incident-energy region of 4−7 MeV in the ^{3}He + p scattering [11], but no resonant behavior is observed in the two S-wave phase shifts with 0^+ and 1^+. The $3N + N$ scattering was previously investigated by various approaches with both realistic [12–15] and effective interactions [3]. The phase shifts, analyzing powers, and cross sections of both ^{3}He + p and ^{3}H + n elastic scatterings were calculated with the RGM in Ref. [15]. In the present article, we will clarify the role of the $d + 2p$ channel in the ^{3}He + p phase shifts by comparing the results by the two different N-N interactions.

We have employed the microscopic cluster model as formulated by the RGM [1]. In this method, all the nucleons are treated explicitly and they are assumed to be arranged in several clusters. The wave function consisting of two clusters $(A + B)$ is given as

$$\Psi_{AB}^{JM\pi} = \sum_{i=1}^{N_A} \sum_{j=1}^{N_B} \sum_{I,\ell} \mathcal{A}\left\{\left[\left[\Phi_{I_A,\pi_A}^{A,i} \Phi_{I_B,\pi_B}^{B,j}\right]_I \chi_\ell(\boldsymbol{\rho})\right]_{JM}\right\}, \quad (1)$$

*arai@nagaoka-ct.ac.jp
†aoyama@cc.niigata-u.ac.jp
‡suzuki@nt.sc.niigata-u.ac.jp

where $\Phi^{A,i}_{I_A,\pi_A}$ and $\Phi^{B,j}_{I_B,\pi_B}$ are the intrinsic wave functions of the clusters A and B, and their spins, I_A and I_B, are coupled to the channel spin I as indicated by the square brackets. The symbol N_A (N_B) stands for the number of the basis set for the cluster intrinsic wave function of the cluster A (B). The first state with i (j) $= 1$ is the ground state and the states with i (j) $\geqslant 2$ denote the so-called "pseudostates," which are constructed by the diagonalization of the Hamiltonian for each cluster. These pseudostates are the discretized continuum states and are necessary to take into account the distortion effects of the scattering clusters [16]. The ground states of ^{3}He and d are bound states but that of the $2p$ (diproton) cluster is a virtual state. The cluster relative motion function $\chi_\ell(\boldsymbol{\rho})$ with the partial wave ℓ is specified by the cluster relative distance coordinate $\boldsymbol{\rho}$. The partial waves ℓ are taken up to $\ell = 3$ at the present calculation. The total wave function in Eq. (1) is properly antisymmetrized as indicated by the intercluster antisymmetrizer $\mathcal{A}$. It contains no center-of-mass wave function and has good total angular momentum JM and parity π.

The combination of clusters included are $(A, B) = (^3\mathrm{He}, p)$ and $(d, 2p)$. Furthermore, we should mention that we take into account not only a simple $[^3\mathrm{He} + p] + [d + 2p]$ coupled channel but also the other possible inelastic channels. In other words, the different spin-parity states of ^{3}He and their pseudostates are included in the $^3\mathrm{He} + p$ channels. Also, for the $d + 2p$ channel, an excited state of the deuteron $d^*(0^+)$ and the pseudostates of d (d^*) and $2p$ clusters are included. These pseudostates, when they are included in the phase-shift calculation, are expected to take account of the distortion of the clusters of the entrance channel [16].

The intrinsic wave functions of ^{3}He used in Eq. (1) are given by the $p + p + n$ three-body calculation,

$$\Phi^{A,i}_{I_A,\pi_A}(^3\mathrm{He}) = \sum_{\lambda_A} C^i_{\lambda_A} \mathcal{A}\left\{\left[\chi_{S_A T_A}\left[\Gamma_{\ell_1}(\nu_1, \boldsymbol{\rho}_1)\Gamma_{\ell_2}(\nu_2, \boldsymbol{\rho}_2)\right]_{L_A}\right]_{I_A}\right\}. \quad (2)$$

The subscript λ_A stands for a set of the labels $\{S_A, T_A, L_A, \ell_1, \ell_2, \nu_1, \nu_2\}$ and $C^i_{\lambda_A}$ are the coefficients of the ith eigenstate obtained by diagonalizing the $p + p + n$ Hamiltonian. The Gaussian basis function $\Gamma_{\ell_i}(\nu_i, \boldsymbol{\rho}_i)$ are given in Eqs. (4) and (5) of Ref. [17] and $\boldsymbol{\rho}_1$, $\boldsymbol{\rho}_2$ are the Jacobi coordinates in the $p + p + n$ system with ℓ_1, ℓ_2 denoting the corresponding orbital angular momenta. The function χ_{S_A,T_A} is the spin and isospin part of ^{3}He with S_A and T_A being the total spin and total isospin, respectively. The total angular momentum and parity ($I^{\pi_A}_A$) of ^{3}He is taken into account up to $5/2^\pm$ with the restriction of ℓ_1, $\ell_2 \leqslant 2$ and $S_A = 1/2$ or $3/2$ and $T_A = 1/2$.

The deuteron wave function has a form similar to that of Eq. (2),

$$\Phi^{A,i}_{I_A,\pi_A}(d) = \sum_{\lambda_A}^{N_A} C^i_{\lambda_A} \mathcal{A}\left\{\left[\chi_{S_A T_A}\Gamma_{L_A}(\nu_1, \boldsymbol{\rho}_1)\right]_{I_A}\right\}, \quad (3)$$

where $I^{\pi_A}_A = 1^+$ with $S_A = 1$, $T_A = 0$, and $L_A = 0$ or 2. We also consider the excited deuteron clusters which have $I^{\pi_A}_A = 0^+$ with $S_A = 0$, $T_A = 1$, and $L_A = 0$. The $2p$ clusters are given similarly to Eq. (3) with $I^{\pi_B}_B = 0^+$ ($S_B = 0$, $T_B = 1$, $L_B = 0$), which is nothing but the isobaric analog state of the excited deuteron mentioned previously. The spatial parts of the cluster wave functions are given in terms of a combination of Gaussian basis functions with different values of ν_1.

The wave functions given in Eqs. (1)–(3) are obtained by solving the respective $A(=2 \sim 4)$ nucleons Schrödinger equation with the Hamiltonian

$$H = \sum_{i=1}^{A} T_i - T_{\mathrm{c.m.}} + \sum_{i<j}^{A} V_{ij}, \quad (4)$$

where T_i is the kinetic energy of the ith nucleon, $T_{\mathrm{c.m.}}$ is the kinetic energy of the center-of-mass motion, and V_{ij} is the nucleon-nucleon interaction.

The cluster relative motion $\chi_\ell(\boldsymbol{\rho})$ in Eq. (1) is solved with the microscopic R-matrix method (MRM) [18], in which the configuration space for the relative motion between the clusters is divided into two regions, inner and outer, by a channel radius. The relative wave function in the inner region is approximated with a superposition of Gaussian basis functions $\Gamma_\ell(\nu, \boldsymbol{\rho})$ with various range parameters ν [17]. The same set of Gaussian basis functions is employed for all the channels. The range parameters are taken in the range of 0.1 fm $< b(=1/\sqrt{\nu}) <$ 15 fm. And the number of ν and the channel radius are determined by the convergence of the calculated phase-shift. To avoid the numerical instability in the MRM calculation, the range parameters in Eqs. (2) and (3) for the cluster intrinsic motion are taken in the range of $b_i(= 1/\sqrt{\nu_i}) < 5$ fm. The relative wave function in the inner region is connected, at the channel radius, smoothly to the asymptotic form of the relative wave function, which is expressed in terms of the Coulomb functions and the scattering S-matrix to be determined.

The MN potential with $u = 0.98$ is employed as the effective N-N interaction. This interaction can reproduce scattering lengths and effective ranges for the two-nucleons S-wave state and fairly well reproduces the binding energies of d, ^{3}H, and ^{4}He [7]. With the spin-orbit term of Reichstein and Tang (set IV) [19], this potential can reproduce low-energy $\alpha + n$ phase shifts for the S and P waves [20].

Figures 1 and 2 display the P- and S-wave elastic scattering phase shifts obtained with the MN potential. The ^{3}He cluster wave function is given by the 15 basis functions that are selected by the SVM. The obtained ^{3}He energy is -7.70 MeV and the root mean square (rms) radius is 1.73 fm. The deuteron wave function is given by four Gaussian basis sets where the Gaussian parameters ν_1 in Eq. (3) are 1.297, 0.552, 0.198, and 0.040 fm^{-2}. The obtained deuteron energy is -2.10 MeV and the rms radius is 1.63 fm, compared to the fully converged values, -2.20 MeV and 1.95 fm, respectively [7]. The basis set for the 0^+ states of the pn and pp clusters are chosen as the same basis functions within a bound-state approximation. The calculated phase shifts with the $^3\mathrm{He} + p$ single channel are shown by the solid lines, and those including additionally the $d + 2p$ channel are shown by the dashed lines. In this calculation, the ^{3}He, d, and $2p$ clusters have only the S-wave component. We see that the $d + 2p$ channel increases the P-wave phase shifts at most 10° and gives the negligible

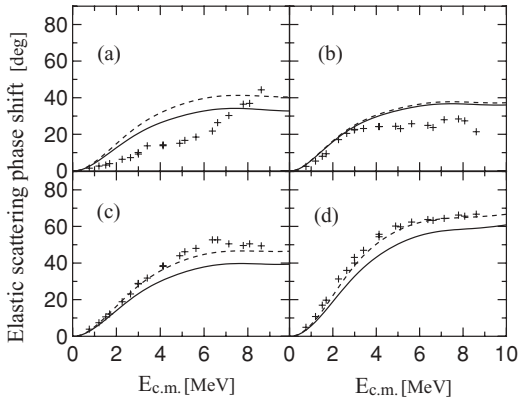

FIG. 1. The $^3\mathrm{He}+p$ P-wave elastic scattering phase shifts of (a) 0^-, (b) $1^-(I=0)$, (c) $1^-(I=1)$, and (d) 2^- states calculated with the MN potential. Here I is the channel spin. The solid and dashed lines denote the results of the $^3\mathrm{He}(1/2^+)+p$ and $[^3\mathrm{He}(1/2^+)+p]+[d(0^+,1^+)+2p(0^+)]$ configurations, respectively. The crosses denote the experimental data [21] and the error bars of the data are omitted.

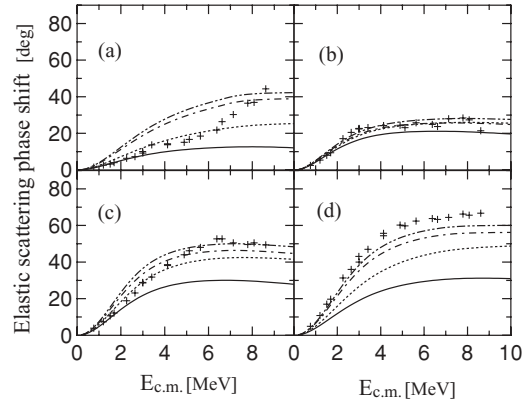

FIG. 3. The $^3\mathrm{He}+p$ P-wave elastic scattering phase shifts of (a) 0^-, (b) $1^-(I=0)$, (c) $1^-(I=1)$, and (d) 2^- states calculated with the AV8′ potential. The lines denote the results obtained including the following configurations: solid, $^3\mathrm{He}(1/2^+)+p$; dotted, $^3\mathrm{He}(1/2^\pm,3/2^\pm,5/2^\pm)+p$; dash-dotted, $[^3\mathrm{He}(1/2^+)+p]+[d(0^+,1^+)+2p(0^+)]$; dash-dot-dotted $[^3\mathrm{He}(1/2^\pm,3/2^\pm,5/2^\pm)+p]+[d(0^+,1^+)+2p(0^+)]$. The crosses denote the experimental data [21] and the error bars of the data are omitted.

contribution on the S-wave phase shifts. Thus, we conclude that the $d+2p$ channel plays a minor role on both the resonant P-wave phase shifts and the nonresonant S-wave phase shifts as far as the conventional effective N-N interaction is used in the cluster model calculation.

We should mention that the conventional microscopic cluster model usually employs a simple $0s$ h.o. wave function for the ^{3}H, ^{3}He, and ^{4}He clusters. When the $(0s)^3$ h.o. wave function is employed for the ^{3}He cluster in the $^3\mathrm{He}+p$ calculation, the $d+2p$ channel gives a considerable contribution on not only the P-wave but also the S-wave phase shifts. These significant differences are attributable to the fact that the $^3\mathrm{He}+p$ and $d+2p$ channels have a large overlap at the short distance of the cluster separation. The inclusion of the $d+2p$ channel plays the role of the distortion effect in the ^{3}He cluster and improves the ^{3}He wave function indirectly. However, once the improved wave function of the ^{3}He cluster is employed, the $d+2p$ channel is strongly suppressed, as seen in Figs. 1 and 2.

A similar suppression by the improvement of the cluster wave function was noted in understanding the neutron-halo structure of ^{6}He in the $\alpha+n+n$ cluster model. As was shown in Refs. [20,22], the use of the simple $(0s)^4$ h.o. function for the α particle led to the conclusion that the $t+t$ channel is really important in gaining the binding energy of ^{6}He. However, if the simple $(0s)^4$ h.o. wave function is replaced with the better one calculated in the $3N+N$ two-body model, the effect of the $t+t$ channel is reduced to a large extent. We have to perform the multiconfiguration calculation, paying due attention to the cluster intrinsic function to evaluate properly the contribution by the other configurations such as the $d+2p$ channel in ^{4}Li.

Figures 3 and 4 display the P- and S-wave phase shifts with the AV8′ potential. The ^{3}He cluster wave function is given by the 15 basis functions selected by the SVM and this wave function gives the ^{3}He energy as -6.27 MeV and the rms radius as 1.73 fm. The states other than $J^\pi=1/2^+$ are given by 10 basis functions within a bound-state approximation. The deuteron wave function is given by six Gaussian basis sets with $\nu_1=2.86$, 0.277, and 0.040 fm^{-2} for the S wave and 1.46, 0.470, and 0.123 fm^{-2} for the D wave. The obtained deuteron energy is -2.03 MeV and the rms radius is 1.70 fm. These three S-wave basis sets are employed for the 0^+ states of the pn and pp clusters within a bound-state approximation. The preceding ground-state properties are compared to the converged results [7]: -7.10 MeV and 1.78 fm for ^{3}He, -2.24 MeV and 1.96 fm for d. We have to limit the number of basis sets

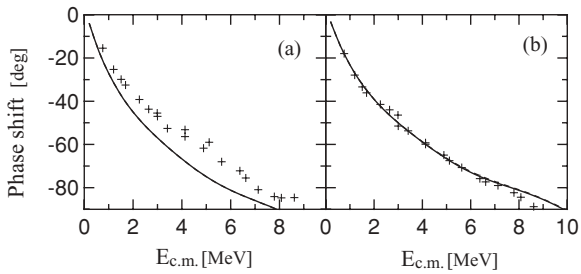

FIG. 2. The $^3\mathrm{He}+p$ S-wave elastic scattering phase shifts of (a) 0^+ and (b) 1^+ states calculated with the MN potential.

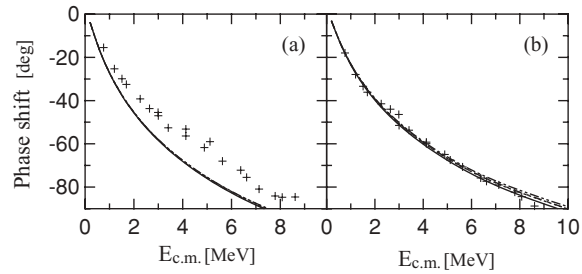

FIG. 4. The $^3\mathrm{He}+p$ S-wave elastic scattering phase shifts of (a) 0^+ and (b) 1^+ states calculated with the AV8′ potential.

for ^{3}He and d clusters to perform the full channel MRM calculation.

Plotted lines in these figures are the phase shifts calculated in the single channel (solid), those including other spin-parity states of ^{3}He (dotted), those including the $d + 2p$ channel (dash-dotted), and those including all of these channels (dash-dot-dotted). With the AV8′ potential, we can see the significant contribution of the $d + 2p$ channel on the P-wave phase shifts. The role of this channel is larger than that of the excited states of ^{3}He, which give only a small contribution when the $d + 2p$ channel is already taken into account. These are quite different from the MN potential case. In contrast to the P-wave phase shifts, the S-wave phase shifts are reasonably well reproduced by the single-channel calculation and these are are quite similar to the results with the MN potential. We verified that this basis truncation does not change our conclusion by comparing to an extended basis calculation. The extended basis uses 30 and 8 Gaussians for ^{3}He and d, respectively, leading to the result close to the converged energy and rms radius. Both basis sets give almost the same phase shifts in the single $[^3\mathrm{He}(1/2^+) + p]$ calculation. The phase shift difference between both sets is less than 5° in the coupled $[^3\mathrm{He}(1/2^+) + p] + [d + 2p]$ calculation. Therefore, the basis truncation does not change our present conclusion.

In conclusion, the ^{3}He + p single-channel calculation with the effective N-N interaction can sufficiently reproduce not only the P-wave phase shifts but also the S-wave phase shifts. On the contrary, the single-channel calculation with the realistic N-N interaction fails to reproduce the P-wave resonant phase shifts and we should take into account the various configurations while the nonresonant S-wave phase shifts can be fairly well reproduced by the single channel. Recently, the $\alpha + N$ phase shifts have been calculated with the realistic N-N interaction [8,23,24]. It is interesting to investigate the role of the additional $t + d$ or some distorted configurations on the resonant P-wave phase shifts to evaluate correctly the contribution of the three-body force.

This work presents research results of Bilateral Joint Research Projects of the JSPS (Japan) and the FNRS (Belgium). This work is supported in part by the Uchida Science Promotion Foundation.

[1] K. Wildermuth and Y. C. Tang, *A Unified Theory of the Nucleus* (Vieweg, Braunschweig, 1977).
[2] D. R. Thompson, M. LeMere, and Y. C. Tang, Nucl. Phys. **A286**, 53 (1977).
[3] H. Furutani, H. Horiuchi, and R. Tamagaki, Prog. Theor. Phys. **62**, 981 (1979).
[4] A. Csótó and R. G. Lovas, Phys. Rev. C **46**, 576 (1992).
[5] B. S. Pudliner, V. R. Pandharipande, J. Carlson, S. C. Pieper, and R. B. Wiringa, Phys. Rev. C **56**, 1720 (1997).
[6] H. Kamada *et al.*, Phys. Rev. C **64**, 044001 (2001).
[7] Y. Suzuki, W. Horiuchi, M. Orabi, and K. Arai, Few-Body Syst. **42**, 33 (2008).
[8] S. Quaglioni and P. Navrátil, Phys. Rev. Lett. **101**, 092501 (2008); Phys. Rev. C **79**, 044606 (2009).
[9] V. I. Kukulin and V. M. Krasnopol'sky, J. Phys. G **3**, 795 (1977).
[10] K. Varga, Y. Suzuki, and R. G. Lovas, Nucl. Phys. **A571**, 447 (1994).
[11] D. R. Tilley, H. R. Weller, and G. M. Hale, Nucl. Phys. **A541**, 1 (1992).
[12] A. Deltuva and A. C. Fonseca, Phys. Rev. C **75**, 014005 (2007); Phys. Rev. Lett. **98**, 162502 (2007).
[13] M. Viviani, A. Kievsky, L. Girlanda, and L. E. Marcucci, arXiv:0812.3547.
[14] R. Lazauskas, Phys. Rev. C **79**, 054007 (2009).
[15] B. Pfitzinger, H. M. Hofmann, and G. M. Hale, Phys. Rev. C **64**, 044003 (2001); C. Reiß and H. M. Hofmann, Nucl. Phys. **A716**, 107 (2003).
[16] H. Kanada, T. Kaneko, S. Saito, and Y. C. Tang, Nucl. Phys. **A444**, 209 (1985).
[17] K. Arai, P. Descouvemont, and D. Baye, Phys. Rev. C **63**, 044611 (2001).
[18] D. Baye, P.-H. Heenen, and M. Libert-Heinemann, Nucl. Phys. **A291**, 230 (1977).
[19] I. Reichstein and Y. C. Tang, Nucl. Phys. **158**, 529 (1970).
[20] A. Csótó, Phys. Rev. C **48**, 165 (1993).
[21] T. A. Tombrello, Phys. Rev. **138**, B40 (1965).
[22] K. Arai, Y. Suzuki, and R. G. Lovas, Phys. Rev. C **59**, 1432 (1999).
[23] Y. Suzuki, W. Horiuchi, and K. Arai, Nucl. Phys. **A823**, 1 (2009).
[24] K. M. Nollett, S. C. Pieper, R. B. Wiringa, J. Carlson, and G. M. Hale, Phys. Rev. Lett. **99**, 022502 (2007).